doi:10.1093/brain/awt184 Brain 2013: 136; 2717–2726 | 2717

BRAIN
A JOURNAL OF NEUROLOGY

# Incident lacunes preferentially localize to the edge of white matter hyperintensities: insights into the pathophysiology of cerebral small vessel disease

**Marco Duering,[1] Endy Csanadi,[1,2] Benno Gesierich,[1] Eric Jouvent,[3] Dominique Hervé,[3] Stephan Seiler,[4] Boubakeur Belaroussi,[5] Stefan Ropele,[4] Reinhold Schmidt,[4] Hugues Chabriat[3] and Martin Dichgans[1,6,7]**

1 Institute for Stroke and Dementia Research, Klinikum der Universität München, Ludwig-Maximilians-University, Marchioninistraße 15, 81377 Munich, Germany
2 Department of Neurology, Klinikum der Universität München, Ludwig-Maximilians-University, Marchioninistraße 15, 81377 Munich, Germany
3 Department of Neurology, CHU Lariboisière, Assistance Publique des Hôpitaux de Paris, 2 rue Ambroise – Paré, 75475 Paris, France
4 Department of Neurology, Medical University of Graz, Auenbruggerplatz 22, 8036 Graz, Austria
5 Bioclinica SAS, 60 Avenue Rockefeller, 69008 Lyon, France
6 German Centre for Neurodegenerative Diseases (DZNE, Munich), Schillerstraße 44, 80336 Munich, Germany
7 Munich Cluster for Systems Neurology (SyNergy), Munich, Germany

Correspondence to: Martin Dichgans, MD
Institute for Stroke and Dementia Research,
Marchioninistraße 15,
81377 Munich,
Germany
E-mail: martin.dichgans@med.uni-muenchen.de

**White matter hyperintensities and lacunes are among the most frequent abnormalities on brain magnetic resonance imaging. They are commonly related to cerebral small vessel disease and associated with both stroke and dementia. We examined the spatial relationships between incident lacunes and white matter hyperintensities and related these findings to information on vascular anatomy to study possible mechanistic links between the two lesion types. Two hundred and seventy-six patients with cerebral autosomal dominant arteriopathy with subcortical infarcts and leukoencephalopathy (CADASIL), a genetically defined small vessel disease with mutations in the *NOTCH3* gene were followed with magnetic resonance imaging over a total of 633 patient years. Using difference images and Jacobian maps from registered images we identified 104 incident lacunes. The majority ($n = 95$; 91.3%) of lacunes developed at the edge of a white matter hyperintensity whereas few lacunes were found to develop fully within ($n = 6$; 5.8%) or outside ($n = 3$; 2.9%) white matter hyperintensities. Adding information on vascular anatomy revealed that the majority of incident lacunes developed proximal to a white matter hyperintensity along the course of perforating vessels supplying the respective brain region. We further studied the spatial relationship between prevalent lacunes and white matter hyperintensities both in 365 patients with CADASIL and in 588 elderly subjects from the Austrian Stroke Prevention Study. The results were consistent with the results for incident lacunes. Lesion prevalence maps in different disease stages showed a spread of lesions towards subcortical regions in both cohorts. Our findings suggest that the mechanisms of lacunes and white matter hyperintensities are intimately connected and identify the edge of white matter hyperintensities as a predilection site for lacunes. Our observations further support and refine the concept of the white matter hyperintensity penumbra.**

Received March 13, 2013. Revised May 19, 2013. Accepted May 24, 2013. Advance Access publication July 17, 2013

**Keywords:** cerebral small vessel disease; small vessel stroke; white matter hyperintensities; lacunes; pathomechanisms

**Abbreviations:** ASPS = Austrian Stroke Prevention Study; CADASIL = cerebral autosomal dominant arteriopathy with subcortical infarcts and leukoencephalopathy

# Introduction

Cerebral small vessel disease is a major cause of both stroke and age-related disability and the most common cause of vascular cognitive impairment (O'Brien *et al*., 2003; Pantoni, 2010). Prominent manifestations of small vessel disease on neuroimaging include $T_2$ hyperintense signals predominantly in the white matter (white matter hyperintensities) and lacunes. Lacunes are small subcortical cavities with an MRI signal identical to CSF.

The mechanisms underlying white matter hyperintensities and lacunes are still very much debated. Lack of progress in this area represents an obstacle to the development of novel diagnostic and therapeutic tools. Traditionally, lacunes are considered to result from occlusion of a single perforating artery (Bamford and Warlow, 1988; Bailey *et al*., 2012) whereas white matter hyperintensities are frequently attributed to chronic hypoperfusion (Fazekas *et al*., 1993; Pantoni and Garcia, 1997; O'Sullivan *et al*., 2002; Schmidt *et al*., 2007). However, this concept has been challenged. Some authors propose that the mechanisms underlying lacunes and white matter hyperintensities might overlap and that their pathogenesis is more intimately connected (Wardlaw *et al*., 2003; Potter *et al*., 2010). This should be reflected in the spatial relationships between newly developing (i.e. incident) lacunes and white matter hyperintensities during lesion evolution.

Studying the spatial relationships between incident lacunes and white matter hyperintensities poses methodological challenges. First, such investigations require longitudinal data to identify incident lesions and study lesion progression. Second, the incidence rate of lacunes is typically very low both in the general population (Vermeer *et al*., 2003) and in subjects with manifestations of cerebral small vessel disease thus requiring large sample sizes and long periods of follow-up. Third, there are competing causes of lacunes aside from cerebral small vessel disease including parent artery occlusion from local atheroma as well as embolism from atherosclerotic lesions or cardiac sources (Wardlaw *et al*., 2013). Autopsy studies have limited utility in studying the evolution of small vessel-related lesions. This is because these lesions rarely cause death thus resulting in considerable delays until histopathological examination. Neuroimaging in combination with dedicated post-processing tools allows for the studying of large cohorts, identifying incident lesions and studying their progression over time.

In the current study we examined possible mechanistic links between small vessel disease-related lesions by investigating the spatial relationships between incident lacunes and pre-existing white matter hyperintensities and by studying the evolution of white matter hyperintensities in parallel with the development of lacunes. We further integrated our findings with knowledge on vessel anatomy. To overcome some of the methodological challenges we studied a large cohort of subjects with genetically defined small vessel disease that was followed over an extended time period using serial MRI. This enabled us to systematically assess a large number of incident lacunes clearly attributable to cerebral small vessel disease. To address the generalizability of our findings towards age-related small vessel disease we further studied prevalent lacunes in a large cohort of community-dwelling middle-aged and elderly subjects.

# Materials and methods

## Study cohorts

The main study cohort included 365 subjects with cerebral autosomal dominant arteriopathy with subcortical infarcts and leukoencephalopathy (CADASIL) recruited through a prospective two-centre study (Klinikum Großhadern, University of Munich, Germany and Hopital Lariboisière, Paris, France) (Jouvent *et al*., 2008; Zieren *et al*., 2013). CADASIL had been confirmed either by skin biopsy or by genetic testing (Joutel *et al*., 1996; Peters *et al*., 2005). Follow-up visits were scheduled at 18, 36 and 54 months. Two hundred and seventy-six subjects had at least one follow-up and were thus included in the longitudinal analysis (Table 1). One hundred and forty subjects had two follow-ups and 53 subjects completed all three follow-ups.

The second sample included a community-dwelling, cross-sectional cohort of 588 elderly subjects from the Austrian Stroke Prevention Study (ASPS) (Schmidt *et al*., 2003, 2005). The ethics committees of all participating institutions approved the study. Written and informed consent was obtained from all subjects.

## Magnetic resonance imaging

We obtained a total of 887 MRI scans in subjects with CADASIL, all of whom had been scanned on 1.5 T systems [Siemens Vision (Munich, $n = 56$) or General Electric Medical Systems Signa (Paris, $n = 588$; Munich, $n = 243$)]. Scans from community-dwelling elderly subjects ($n = 588$) were drawn from the Austrian Stroke Prevention Study (ASPS) (Schmidt *et al*., 1999). A subgroup of 367 subjects within ASPS underwent scanning on a 3 T system including a 1 $mm^3$ isotropic resolution 3D $T_1$. Sequence parameters are given in Supplementary Table 3. Of note, all subcortical hyperintense lesions on FLAIR images were deemed white matter hyperintensities, regardless of whether they occurred in white or subcortical grey matter. Thus, hyperintensities located in the basal ganglia were also named white matter hyperintensities.

## Identification of incident and prevalent lacunes

Incident lacunes were identified using difference imaging and Jacobian maps (Fig. 1) from 3D $T_1$ images at different time points (Duering *et al*., 2012*b*). All follow-up images were registered to the baseline scans using a mutual information-based algorithm (Mattes *et al*., 2001). After intensity normalization (Lewis and Fox, 2004) difference

**Table 1 Characteristics of the CADASIL cohort with available follow-up MRI scans (*n* = 276)**

| | Total (*n* = 276) | Incident lacunes (*n* = 64) | No incident lacunes (*n* = 212) | *P*-value |
|---|---|---|---|---|
| **Demographic characteristics** | | | | |
| Age, mean (range) [years] | 49.9 (22.9–77.4) | 52.1 (34.6–72.4) | 49.2 (22.9–77.4) | 0.046 |
| Female sex, *n* (%) | 150 (54.3) | 30 (46.9) | 120 (56.6) | 0.197 |
| **Vascular risk factors** | | | | |
| Hypertension, *n* (%) | 49 (17.8) | 10 (15.6) | 39 (18.4) | 0.711 |
| Hypercholesterolaemia, *n* (%) | 108 (39.1) | 30 (46.9) | 78 (36.8) | 0.188 |
| Smoking, *n* (%) | 151 (54.7) | 39 (60.9) | 112 (52.8) | 0.316 |
| Diabetes, *n* (%) | 6 (2.17) | 2 (3.13) | 4 (1.89) | 0.626 |
| **Imaging characteristics** | | | | |
| WMHV, median (IQR) [ml] | 83.3 (90.5) | 96.1 (94.2) | 80.0 (87.0) | $5.92 \times 10^{-3}$ |
| Normalized WMHV*, median (IQR) [%] | 6.02 (6.72) | 6.95 (6.33) | 5.58 (6.75) | $8.59 \times 10^{-3}$ |
| Lacune volume, median (range) [μl] | 92.4 (0-624) | 439 (0-515) | 47.8 (0-624) | $8.78 \times 10^{-8}$ |
| Normalized lacune volume*, median (IQR) [%] | 0.00703 (0.0310) | 0.0311 (0.0479) | 0.00322 (0.0204) | $7.32 \times 10^{-8}$ |
| Number of lacunes, median (IQR) | 2 (7) | 6 (7) | 1 (5) | $3.22 \times 10^{-7}$ |

WMHV = white matter hyperintensity volume.
*Normalization was achieved by dividing lesion volume through the volume of the intracranial cavity.

images were obtained by subtracting the preprocessed follow-up $T_1$ image from the $T_1$ image at study inclusion. Jacobian images were obtained by taking the determinant of the Jacobian matrices of each voxel after non-linear warping of the preprocessed follow-up image to the image at study inclusion (Calmon *et al*., 1998; Vemuri *et al*., 2003).

Prevalent lacunes were identified on 3D $T_1$ images with 1 mm isotropic resolution and defined as cystic lesions with a signal identical to CSF in $T_1$- and $T_2$-weighted images. Both incident and prevalent lesions were thoroughly examined to distinguish lacunes from enlarged perivascular Virchow-Robin spaces using well-established criteria including size (>2 mm diameter for lacunes), shape, location and the typical orientation of perivascular spaces along the course of perforating vessels (Herve *et al*., 2005; Doubal *et al*., 2010*a*; Zhu *et al*., 2011). Using these criteria, an excellent intra- and inter-rater reliability (two raters) was achieved as judged by a Cohen's kappa value of >0.95.

## Visual rating of the spatial relationships between lesions

To determine the spatial relationship between incident lacunes and pre-existing white matter hyperintensities as well as white matter hyperintensities developing in parallel to lacunes, we used a visual rating scale (Fig. 2). We analysed all incident lacunes that occurred in the cerebral hemispheres (see Table 2 for an overview of incident lacunes locations). Baseline analyses were performed individually for every incident lacune on the last scan before its appearance. Incident lacunes were rated for their location with regard to pre-existing white matter hyperintensities using the following categories: no contact (grade 0), contact without overlap (grade Ia), partial overlap (grade Ib), and complete overlap (grade II) with a pre-existing white matter hyperintensity. Importantly, all ratings were done by a reader unaware of the study hypothesis. On follow-up scans, small $T_2$-hyperintensity rims around incident lacunes were not regarded as white matter hyperintensities. Inter-rater reliability (between two raters) was very good as judged by Cohen's kappa values >0.9. There was no significant difference in the distribution of visual rating categories for incident lacunes between the two centres and therefore no indication for a scanner bias or centre effect.

## Relationships with vessel anatomy

Incident lesions in contact (grade Ia) or with partial overlap to white matter hyperintensities (grade Ib) were further rated with regard to their location along perforating arteries. To determine the orientation of perforating arteries within brain regions affected by incident lacunes we used a comprehensive vascular histological atlas (Salamon and Corbaz, 1971). This atlas provides detailed information on the orientation of perforating arteries in different brain regions visualized by post-mortem dye injection in a single human subject. Slices from the atlas in all planes (axial, coronal and sagittal) were inspected side by side with the magnetic resonance images. Considering the course of perforating arteries in the respective brain regions incident lacunes were then graded as being either proximal or distal (in relation to the white matter hyperintensities) along the course of the perforating vessel. This analysis reached good inter-rater reliability (Cohen's kappa 0.87).

## Prevalence maps for white matter hyperintensities and lacunes

For the analysis of the distribution of white matter hyperintensities and lacunes in the cross-sectional cohorts, lesion masks were generated and registered to Montreal Neurological Institute (MNI) 152 standard space. Lesion segmentation procedures have previously been published both for the CADASIL cohort (Duering *et al*., 2012*a*) and the ASPS cohort (Schmidt *et al*., 2005).

In brief, lesion maps in the CADASIL cohort were generated using custom 2D and 3D editing tools from BioClinica SAS using a semi-automated procedure with intensity thresholding and manual corrections. The intra- and inter-rater reliability for these procedures and the Dice coefficient as a measure for overlap between raters has been shown to be high (Schmidt *et al*., 1999; Viswanathan *et al*., 2006, 2010; Duering *et al*., 2011). Read–reread reliability for lesion volumes after switching the scanner at the Munich site was also very high (intraclass correlation coefficient 0.96).

The normalization procedure to MNI 152 space involved tools from the Functional Magnetic Resonance Imaging of the Brain Software Library (Smith *et al*., 2004; Woolrich *et al*., 2009) and incorporated

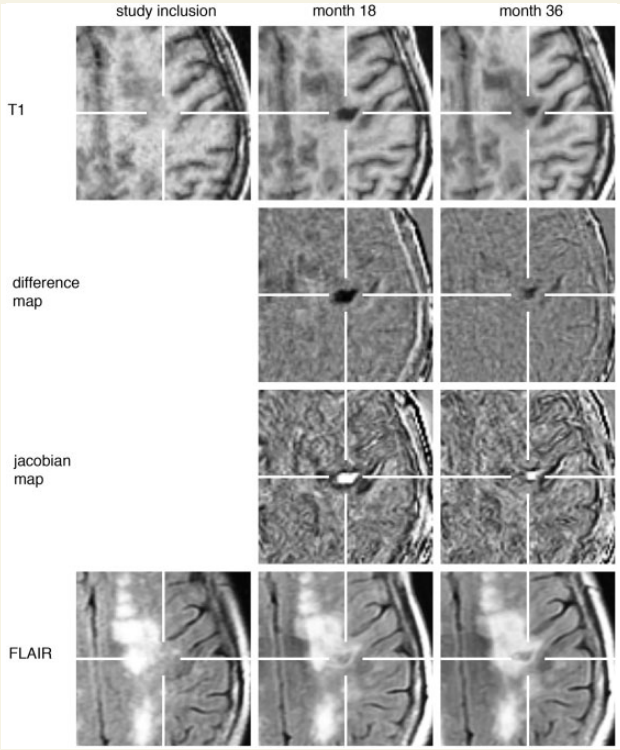


**Figure 1** Identification of incident lacunes. Example of an incident lacune that had occurred between baseline and 18 month follow-up. The incident lacune is easily identified as a dark region on difference maps (bright on the Jacobian maps). Registered FLAIR images are used to determine the relationship with white matter hyperintensities at each time point. This incident lacune was rated as grade Ia (baseline) and I (follow-up) according to the visual rating scale depicted in Fig. 2.

a lesion masking approach (Brett *et al.*, 2001). After quality control 23 subjects from the CADASIL cohort and seven subjects from the ASPS cohort had to be excluded for the following reasons: motion artefacts (CADASIL: $n = 5$; ASPS: $n = 1$), inability to register images to standard space (CADASIL: $n = 13$, ASPS: $n = 4$) and concomitant pathologies, such as large vessel stroke (CADASIL: $n = 5$, ASPS: $n = 1$) and meningioma (CADASIL: $n = 0$, ASPS: $n = 1$).

The final sample for the cross-sectional analysis in standard space consisted of 342 subjects with CADASIL and 581 ASPS subjects. For both cohorts, white matter hyperintensities maps in MNI 152 space were stratified into deciles according to the global lesion volume. Lesion probability maps were calculated in each group to identify predilection sites and to compare the pattern in each disease stage.

## Statistical analysis

All statistical analyses were conducted with the R software package (version 2.13.2) (R Core Team, 2012). We first checked continuous variables for normal distribution using the Shapiro-Wilk test. For group comparisons of normally distributed data, we used the two-tailed Student's *t*-test. The Wilcoxon rank sum test (Mann-Whitney U-test) was used for non-normally distributed data. For group comparisons of binominal data we applied Fisher's exact test.

# Results

## Characteristics of incident lacunes in subjects with CADASIL

We identified a total of 104 incident lacunes (Table 2) in 64 of 276 subjects with CADASIL (mean follow-up = 27.5 months). Forty subjects had a single incident lacunes, 17 had two, and seven had three or more incident lacunes. Compared with subjects without incident lacunes, patients with incident lacunes were older, had higher normalized volumes of both white matter hyperintensities and lacunes and a higher number of prevalent lacunes at baseline (Table 1). Groups were balanced with respect to gender and vascular risk factors. Twenty-one (32.8%) of the 64 patients with incident lacunes had stroke symptoms during follow-up. Thus the majority of incident lacunes were clinically silent.

## Spatial relationship between incident lacunes and white matter hyperintensities

Ninety-five incident lacunes (91.3%) appeared in brain regions showing contact or partial overlap with pre-existing white matter hyperintensities (grade I rated at baseline), 47 of which (45.2%) developed in contact but with no overlap with a pre-existing white matter hyperintensity (grade Ia, Fig. 2) and 48 of which (46.1%) developed in regions showing partial overlap with a pre-existing white matter hyperintensity (grade Ib). Sixty per cent of the latter category (29 of 48) showed an overlap smaller than one-third of the estimated incident lacunes volume.

Only six lesions (5.8%) developed fully inside a pre-existing white matter hyperintensity (grade II) and only three incident lacunes (2.9%) developed in white matter appearing normal on $T_2$/FLAIR-weighted scans at baseline (grade 0). However, in all of the latter cases there was contact with white matter hyperintensities on follow-up scans, as white matter hyperintensities had developed in parallel with the lacunes. Rating examples are provided in Fig. 3. We further calculated the *a priori* probability for each category (Supplementary material). The calculated distribution (grade 0: 34.9%, Ia: 14.5%, Ib: 37.0 %, II: 13.5 %) was significantly different from the observed distribution of the 104 incident lacunes (Chi-squared 46.9, df = 3, $P = 3.57 \times 10^{-10}$).

Overall, 98 incident lacunes (94.2%) showed contact with white matter hyperintensities present either at baseline or developing in parallel with the incident lacunes.

## Progression of white matter hyperintensities in vicinity of incident lacunes

In two cases, white matter hyperintensities progressed in parallel with the appearance of the incident lacunes such that the white matter hyperintensities showed contact at baseline (grade I) and complete overlap (grade II) at follow-up (Fig. 2). Ninety-three

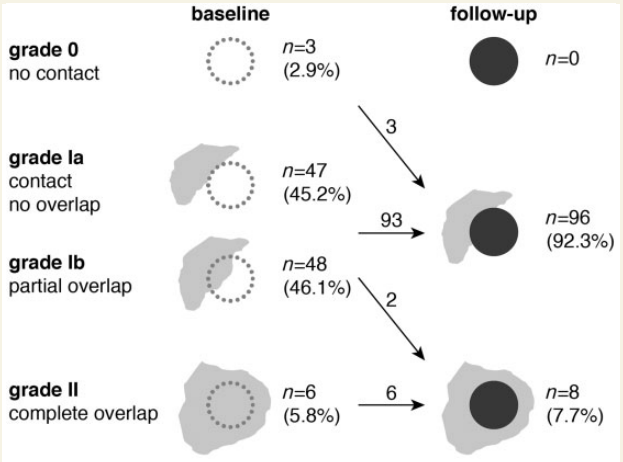


**Figure 2** Visual rating scale. Spatial relationship between incident lacunes and pre-existing white matter hyperintensities rated at baseline (before appearance of the incident lacune) and between incident lacunes and white matter hyperintensities at follow-up. Numbers indicate rating results for the 104 incident lacunes. Arrows indicate changes in the spatial relationships between time points. Note, that there is no distinction between grade Ia and Ib at follow-up because the two categories cannot be distinguished in the presence of a lacune. Small hyperintense rims surrounding incident lacunes on the follow-up scans were not considered as white matter hyperintensities. Such rims were present in 75 incident lacunes (72.1%).

**Table 2 Location of incident lacunes ($n = 104$) in the CADASIL cohort**

| Location | Side | *n* (incident lacunes) |
|---|---|---|
| Basal ganglia | Left | 9 |
| | Right | 6 |
| Centrum semiovale | Left | 21 |
| | Right | 14 |
| Corona radiata | Left | 6 |
| | Right | 5 |
| Corpus callosum | Left | 5 |
| | Right | 1 |
| | Midline | 4 |
| Frontal pole | Left | 9 |
| | Right | 5 |
| Internal capsule | Left | 7 |
| | Right | 4 |
| Occipital pole | Left | 3 |
| | Right | 5 |

lesions remained in partial contact with white matter hyperintensities during follow-up. For these lesions we estimated the spread of white matter hyperintensities in the direction of the incident lesion by estimating the surface coverage by white matter hyperintensities at baseline and at follow-up. An increase in surface coverage was found for 54 lesions (58.0%). In 37 lesions (39.7%) there was no change in surface coverage, whereas a decrease in surface coverage of adjacent white matter hyperintensities was found in two lesions (2.15%).

Thus, a progression of white matter hyperintensities around the incident lesion was detectable in the majority of cases.

## Spatial relationship between incident lacunes and white matter hyperintensities with respect to perforating arteries

Next, we examined the spatial relationships of incident lacunes and white matter hyperintensities with regard to the orientation of perforating arteries by using a comprehensive atlas of vascular territories in the human brain (Salamon and Corbaz, 1971) (Fig. 4A).

Focusing on incident lacunes that developed at the edge of pre-existing white matter hyperintensities (grade I, Fig. 2, $n = 95$), we investigated whether incident lacunes occurred proximal or distal of the white matter hyperintensities with regard to the orientation of perforating arteries in the respective region (Fig. 4B). Again, all readings were done by a rater (E.C.) unaware of any study hypotheses. In 72 cases (76%) the spatial relationships between incident lacunes, pre-existing white matter hyperintensities, and vascular territories could be clearly delineated. Here, the majority of incident lacunes ($n = 70$, 97.2% of classifiable cases) developed proximal to the pre-existing white matter hyperintensities with regard to the origin of the perforating artery. Two incident lacunes (2.8% of classifiable cases) occurred distal of a white matter hyperintensity. Twenty-three (24%) of the 95 lesions were judged not classifiable because the vascular territory could not be clearly delineated (Fig. 4B).

## Spatial relationship between lacunes and white matter hyperintensities in age-related small vessel disease

To address the generalizability of our findings towards age-related small vessel disease we next examined the spatial relationships between lacunes and white matter hyperintensities in the ASPS. Because of the paucity of incident lacunes in ASPS we studied prevalent lacunes. Fourteen of the 367 subjects with suitable scans (3D $T_1$ available) had prevalent lacunes (Supplementary Table 1). All of them were clinically silent and all of them were found at the edge of white matter hyperintensity (grade I, Supplementary Fig. 1).

We also analysed prevalent lacunes in patients with CADASIL. To avoid confounding by confluent white matter hyperintensities in advanced disease stages and to achieve comparability with data from ASPS we analysed patients within the first three deciles of normalized white matter hyperintensities volume. This included 18 subjects with 20 prevalent lacunes (mean normalized white matter hyperintensities volume 2.57%; range 0.537–3.56%, Supplementary Table 2). Seventeen prevalent lacunes (85%) showed the same pattern as in ASPS (grade I). Three lesions showed no contact to white matter hyperintensities (resembling grade 0). All of them were located in the thalamus.

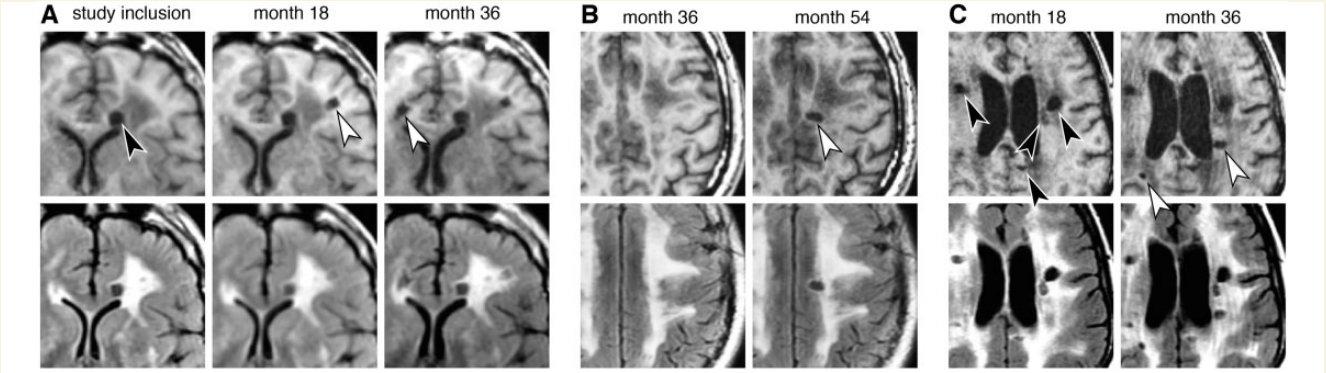


**Figure 3** Rating examples. (**A**) Subject with two incident lacunes that had occurred between study inclusion and Month 18 and between Months 18 and 36, respectively (white arrowheads on $T_1$, *top* row). In addition there is a prevalent (old) lacune visible at study inclusion (black arrowhead). The two incident lacunes were rated as grade Ib at baseline and as grade I at follow-up based on the registered FLAIR images (*bottom* row). (**B**) Example of an incident lacune that had manifested between Months 36 and 54 (white arrowhead). This lesion was rated as grade Ib on the Month 36 scan and as grade I on the Month 54 scan. (**C**) Example of multiple prevalent lacunes (black arrowheads). There is a larger incident lacune developing within a white matter hyperintensity rated as grade II both on the Month 18 and the Month 36 scan. A second, smaller incident lacune corresponding to grade Ib (month 18) and grade I (month 36) is in the right hemisphere.

## Anatomical distribution of white matter hyperintensities and lacunes across disease stages

To examine the spatial progression of lesions across disease stages we generated lesion prevalence maps for white matter hyperintensities and lacunes after dividing the overall sample of subjects with CADASIL into deciles according to white matter hyperintensities volume (Fig. 5A). Visual inspection of the prevalence maps identified the periventricular white matter as the earliest and most prevalent location for white matter hyperintensities. A second prominent cluster emerged somewhat lateral between the external capsule and corona radiata. A third cluster was found in the temporopolar white matter as previously described for patietns with CADASIL. With greater lesion volumes white matter hyperintensities tended to expand towards the subcortical white matter. The prevalence of white matter hyperintensities in ASPS (Fig. 5B) was much lower than in subjects with CADASIL and there were no lesions in the temporopolar white matter. However, there was a similar pattern and spread of lesions with regard to the periventricular and more lateral white matter hyperintensities cluster (Fig. 5B).

The spatial distribution of lacunes in patients with CADASIL differed from the distribution of white matter hyperintensities in that lesions commenced more laterally than the periventricular white matter hyperintensities (first and second decile) and also spread into the ventral parts of the internal capsule and basal ganglia (third to 10th decile). However, lacunes also developed in subcortical regions, particularly in patients with higher white matter hyperintensities volumes (fifth to 10th decile). Because of the low number of prevalent lacunes in ASPS ($n = 14$) we did not generate prevalence maps in this cohort. The location of lacunes in ASPS is detailed in Supplementary Table 1. The observed pattern is in line with the pattern of prevalent lacunes in subjects with CADASIL.

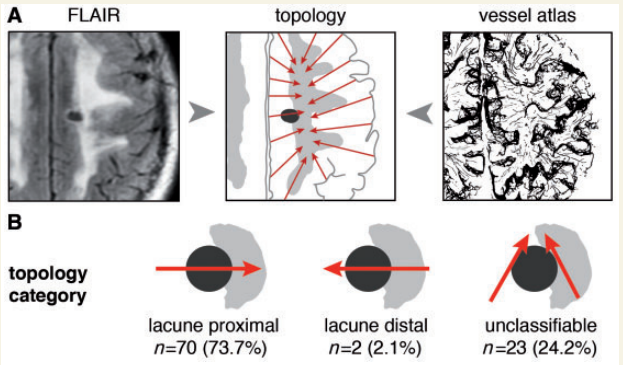


**Figure 4** Topology of incident lacunes, white matter hyperintensities and perforating arteries. (**A**) The topology (*middle* panel) was estimated by integrating information on lesions from FLAIR images (*left* panel) and perforating arteries from the vessel atlas (*right* panel, schematic representation). The axial pane is shown for demonstration purposes. Ratings were done by inspecting images in all planes (axial, coronal and sagittal). (**B**) Incident lacunes were classified in relation to both white matter hyperintensities and the anatomical course of perforating arteries in that region (red arrow). Twenty-three cases could not be classified because of uncertainties in the course of the vessel. The majority of classifiable incident lacunes occurred proximal to the pre-existing white matter hyperintensities with regard to the origin of the perforating artery.

# Discussion

This study provides a detailed account of the spatial relationships between incident lacunes and white matter hyperintensities in a large cohort of subjects with pure small vessel disease while considering information on vascular anatomy. The main

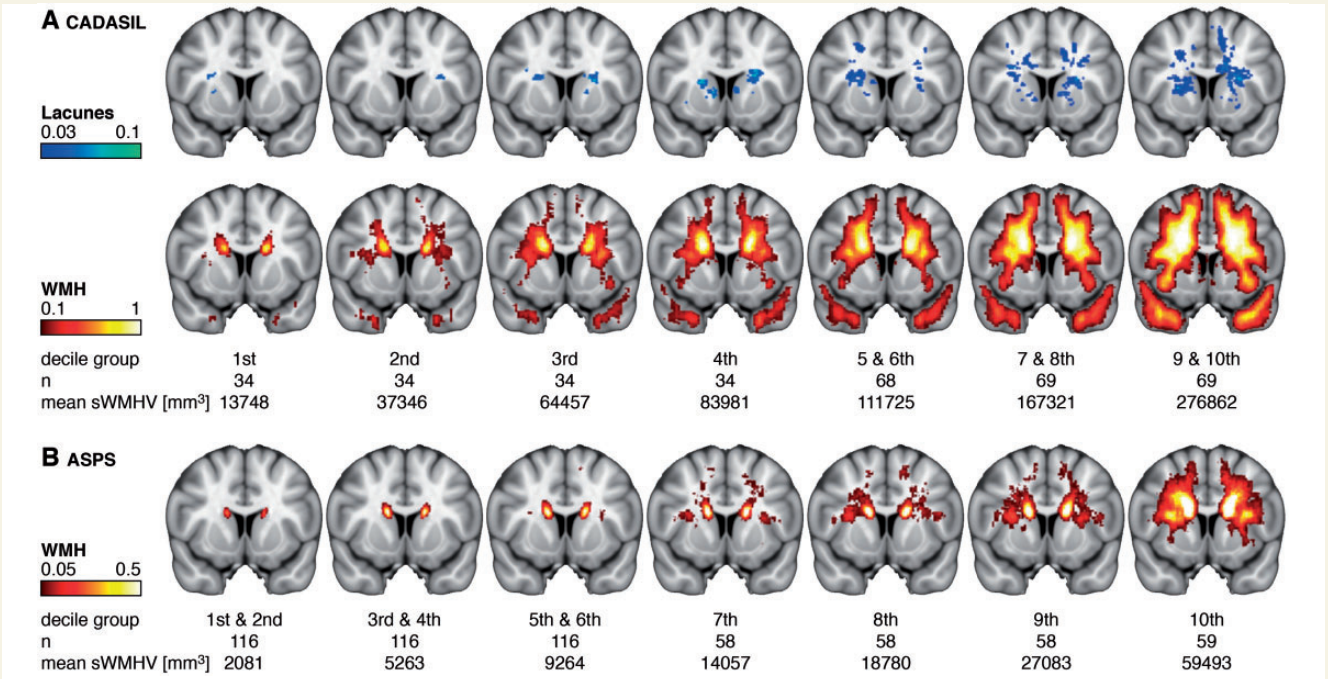


**Figure 5** Lesion probability maps for white matter hyperintensities (WMH) and prevalent lacunes. Lesion masks in standard space for CADASIL ($n = 342$, **A**) and ASPS ($n = 581$, **B**) were summed up after grouping subjects in deciles according to the global white matter hyperintensities volume in standard space (sWMHV). Probability maps for each decile group are superimposed on a coronal section of the MNI 152 $T_1$ template. Note the different scales for CADASIL and ASPS reflecting marked difference in lesion volume.

findings are as follows: (i) the majority of incident lacunes developed at the edge of a white matter hyperintensity and the distribution of prevalent lacunes both in subjects with CADASIL and in subjects with age-related sporadic small vessel disease was consistent with this observation; (ii) in most cases there was a spread of white matter hyperintensities around the incident lacunes during follow-up; and (iii) most incident lacunes developed proximal to white matter hyperintensities with regard to the anatomical course of perforating vessels. Lesion prevalence maps for white matter hyperintensities across different disease stages showed a spread of lesions from the periventricular to subcortical regions in both study cohorts. These findings provide novel insights into the mechanisms of lacunes and white matter hyperintensities as the two most prominent manifestations of small vessel disease.

More than 90% of incident lacunes appeared at the edge of a pre-existing white matter hyperintensity with half of them showing no overlap with the white matter hyperintensity. At follow-up, still >90% of incident lacunes showed partial contact with a white matter hyperintensity, whereas only 7% were fully surrounded by white matter hyperintensities. This finding identifies the edge of white matter hyperintensities as a predilection site for the appearance of cavitating lesions and suggests that the pathophysiology of small vessel disease-related incident lacunes is connected to the pathophysiology of white matter hyperintensities. The conclusion is substantiated by our findings on prevalent lacunes particularly in the ASPS cohort. In ASPS all prevalent lacunes were found to be located at the edge of a white matter hyperintensity despite the fact that the overall amount of white matter hyperintensities and lacunes was relatively small.

Our results are in some contrast to observations from the Leukoaraiosis and Disability (LADIS) study that found incident lacunes to commonly develop either within or outside pre-existing white matter hyperintensities (Gouw *et al*., 2008). However, the results are difficult to compare, as that study included no category for contact or partial overlap, which was the most common location for lacunes in the current study. In LADIS, basal ganglia lacunes were found to be associated with atrial fibrillation thus suggesting cardio-embolism as a cause of lacunes in some of the LADIS patients. The assignment of subcortical ischaemic lesions to specific aetiologies is notoriously difficult because there are various mechanisms apart from small vessel disease including macroatheroma of the parent artery (Kim and Yoon, 2013) and embolism from arterial and cardiac sources (Lammie and Wardlaw, 1999). The current study focused on patients with genetically-defined small vessel disease and there were no competing aetiologies for stroke in our patients with CADASIL. Thus, our findings can be clearly attributed to small vessel disease, in particular CADASIL-related small vessel disease. A common challenge in studying lacunes is differentiating these lesions from enlarged perivascular spaces. In the current study particular care was taken to exclude perivascular spaces by using previously established criteria (Doubal *et al*., 2010*b*). This might in part explain differences between our observations and earlier results.

Our findings shed some light on the mechanisms of lacunes. The proportion of incident lacunes that developed fully within a

pre-existing white matter hyperintensity was low (<6%) suggesting that the conversion of incomplete ischaemic lesions into cystic fluid-filled cavities is a relatively rare mechanism of lacunes at least in our study population. For the most part, incident lacunes appeared in normal appearing brain tissue in proximity to an existing white matter hyperintensity. Recent work suggests that brain tissue neighbouring white matter hyperintensities may be a predilection site for additional ischaemic injury. Thus, for example, a recent diffusion tensor imaging study found subtle alterations of microstructural integrity in tissue surrounding white matter hyperintensities (Maillard *et al*., 2011). This led the authors to propose the term 'white matter hyperintensity penumbra' to characterize tissue at risk of turning into a more severe lesion, and in fact, the same group recently demonstrated that increases in white matter hyperintensities volume are typically driven by the expansion of pre-existing lesions rather than by emergence of new lesions (Maillard *et al*., 2012). In conjunction with the current results, these observations characterize the 'white matter hyperintensity penumbra' as a predilection site for new ischaemic lesions including both white matter hyperintensities and lacunes. Owing to the descriptive nature of our study we are not able to provide more detailed insights into the mechanisms. Yet, our results provide an important starting point for targeted mechanistic investigations including experimental studies in animal models (Shih *et al*., 2013).

Adding information on vessel anatomy we found that in more than 95% of interpretable cases incident lacunes developed proximal to the pre-existing white matter hyperintensities in the course of a perforating vessel. Notably, lacunes do not seem to extend into the vascular end zone. We can only speculate on the reasons for this observation. For one, lacunes may originate from tertiary artery occlusions rather than occlusion of the parent perforator artery itself as suggested in a recent histopathological study that performed intra-arterial dye injections in parallel with an examination of lacunes (Feekes *et al*., 2005). Second, brain regions already affected by white matter hyperintensities might have developed some tolerance to ischaemia due to previous exposure to hypoperfusion (Dirnagl *et al*., 2009).

The lesion prevalence maps for white matter hyperintensities in subjects with CADASIL and elderly participants from ASPS confirm the vascular end zone as a predilection site for white matter hyperintensities. As the disease progresses, white matter hyperintensities typically expand towards the subcortical white matter usually along the trajectories of perforating vessels (Figs 5 and 6). Our results indicate that lacunes typically develop at the edge of expanding white matter hyperintensities, which may subsequently expand up to a degree, where the lacune is fully surrounded by white matter hyperintensities (Fig. 2).

Our study has several methodological strengths including a unique sample of patients with genetically defined small vessel disease and without competing stroke aetiology, the large number of incident lacunes, our approach of using difference images and Jacobian maps for the identification of incident lacunes, the use of co-registered images for the assessment of spatial relationship, and the addition of data on prevalent lacunes from both inherited and age-related small vessel disease. Our methods offer clear advantages over the side-by-side inspection of non-registered scans, which heavily relies on the rater's anatomical skills (Wardlaw, 2008). Importantly, all rating scales reached high intra- and inter-rater reliability.

Limitations include scanning at 1.5 T, the use of different scanners, and the lack of an isotropic 3D FLAIR sequence, which might have facilitated the 3D rating of lesions. Another limitation is the use of a single subject atlas on vascular anatomy (Salamon and Corbaz, 1971) rather than data derived from study participants. However, the principal anatomy of perforating arteries and supply pattern within the brain has been shown to be highly uniform across individuals (Feekes *et al*., 2005) and there are currently no protocols for visualizing the human microvasculature *in vivo*. On average, patients with incident lacunes had higher lesion volumes than those without and there were few patients with incident lacunes that were within early disease stages of CADASIL. Thus, we cannot exclude that the spatial relationships between lesions in less affected individuals are different. Of note, however, our data on prevalent lacunes in subjects with CADASIL with a low volume of white matter hyperintensities are consistent with our findings on incident lacunes.

Ideally, the analysis in ASPS would have been done on incident lesions. However, there were no incident lacunes in community-dwelling subjects from ASPS. The frequency of prevalent lacunes was also quite low as expected in a community-dwelling sample. Of note, none of the subjects in ASPS had a history of stroke. Thus, all lacunes in ASPS were clinically silent. Still, the results match closely with those obtained from incident lacunes in CADASIL. Our observations on prevalent lacunes and the lesion prevalence maps emphasize similarities between CADASIL and age-related small vessel disease and this is also suggested by the similar clinical presentation (Charlton *et al*., 2006; Chabriat *et al*., 2009; Pantoni, 2010). We acknowledge differences such as the earlier age of onset, greater severity of magnetic resonance changes, and involvement of the temporopolar white matter in CADASIL. However, the overall spread of lesions across disease stages was remarkably similar in CADASIL and ASPS and consistent with the concept that lesions commence in periventricular regions and subsequently spread towards the subcortical white matter.

Our findings might have clinical relevance. The principal pattern of white matter hyperintensities and lacunes observed in the current study can be clearly attributed to small vessel disease. Similar studies in patients with other defined aetiologies, such as local atheroma or cardio-embolism are now needed to determine whether the spatial relationship between lacunes and white matter hyperintensities can serve as a diagnostic criterion for distinguishing between different aetiologies.

In conclusion, our data suggest that the mechanisms of lacunes and white matter hyperintensities are intimately connected. Our findings identify the edge of white matter hyperintensities as a predilection site for lacunes and suggest that these lesions typically occur proximal to pre-existing white matter hyperintensities with regard to the anatomical course of perforating vessels. These observations offer insights into the mechanisms underlying white matter hyperintensities and lacunes and refine the concept of the white matter hyperintensity penumbra.

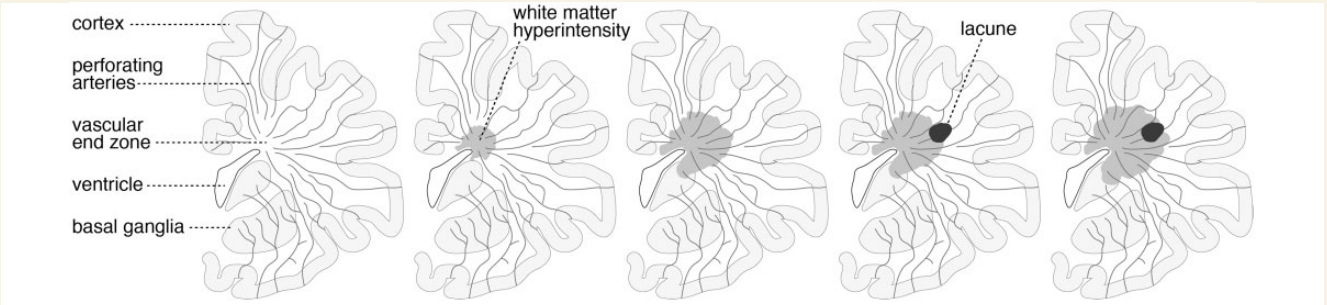


**Figure 6** Proposed model for a typical evolution of white matter hyperintensities and lacunes in small vessel disease. White matter hyperintensities commonly first appear in brain regions corresponding to vascular end zones. They then progress along the more proximal parts of perforating arteries towards the subcortical white matter and the basal ganglia. Lacunes preferentially appear at the edge of white matter hyperintensities, for the most part in brain tissue with normal FLAIR signal on MRI. White matter hyperintensities may expand around lacunes.

# Funding

This work was supported by the Vascular Dementia Research Foundation, the German Centre for Neurodegenerative Diseases (DZNE), an FP6 ERA-NET NEURON grant (01 EW1207), PHRC grant AOR 02-001 (DRC/APHP), Association de Recherché en Neurologie Vasculaire (ARNEVA), Hôpital Lariboisiere, France and by the Austrian Science Fund projects P20103 and I904.

# Supplementary material

Supplementary material is available at *Brain* online.

# References

Bailey EL, Smith C, Sudlow CL, Wardlaw JM. Pathology of lacunar ischemic stroke in humans–a systematic review. Brain Pathol 2012; 22: 583–91.

Bamford JM, Warlow CP. Evolution and testing of the lacunar hypothesis. Stroke 1988; 19: 1074–82.

Brett M, Leff AP, Rorden C, Ashburner J. Spatial normalization of brain images with focal lesions using cost function masking. Neuroimage 2001; 14: 486–500.

Calmon G, Roberts N, Eldridge P, Jean-Philippe T. Automatic quantification of changes in the volume of brain structures. Med Image Comput Comput Assist Interv 1998; 1496: 761–9.

Chabriat H, Joutel A, Dichgans M, Tournier-Lasserve E, Bousser MG. Cadasil. Lancet Neurol 2009; 8: 643–53.

Charlton RA, Morris RG, Nitkunan A, Markus HS. The cognitive profiles of CADASIL and sporadic small vessel disease. Neurology 2006; 66: 1523–6.

Dirnagl U, Becker K, Meisel A. Preconditioning and tolerance against cerebral ischaemia: from experimental strategies to clinical use. Lancet Neurol 2009; 8: 398–412.

Doubal FN, Maclullich AM, Ferguson KJ, Dennis MS, Wardlaw JM. Enlarged perivascular spaces on MRI are a feature of cerebral small vessel disease. Stroke 2010a; 41: 450–4.

Doubal FN, Maclullich AM, Ferguson KJ, Dennis MS, Wardlaw JM. Enlarged perivascular spaces on MRI are a feature of cerebral small vessel disease. Stroke 2010b; 41: 450–4.

Duering M, Zieren N, Herve D, Jouvent E, Reyes S, Peters N, et al. Strategic role of frontal white matter tracts in vascular cognitive impairment: a voxel-based lesion-symptom mapping study in CADASIL. Brain 2011; 134 (Pt 8): 2366–75.

Duering M, Gonik M, Malik R, Zieren N, Reyes S, Jouvent E, et al. Identification of a strategic brain network underlying processing speed deficits in vascular cognitive impairment. Neuroimage 2012a; 66C: 177–83.

Duering M, Righart R, Csanadi E, Jouvent E, Hervé D, Chabriat H, et al. Incident subcortical infarcts induce focal thinning in connected cortical regions. Neurology 2012b; 79: 2025–8.

Fazekas F, Kleinert R, Offenbacher H, Schmidt R, Kleinert G, Payer F, et al. Pathologic correlates of incidental MRI white matter signal hyperintensities. Neurology 1993; 43: 1683–9.

Feekes JA, Hsu SW, Chaloupka JC, Cassell MD. Tertiary microvascular territories define lacunar infarcts in the basal ganglia. Ann Neurol 2005; 58: 18–30.

Gouw AA, van Der Flier WM, Pantoni L, Inzitari D, Erkinjuntti T, Wahlund LO, et al. On the etiology of incident brain lacunes: longitudinal observations from the LADIS study. Stroke 2008; 39: 3083–5.

Herve D, Mangin JF, Molko N, Bousser MG, Chabriat H. Shape and volume of lacunar infarcts: a 3D MRI study in cerebral autosomal dominant arteriopathy with subcortical infarcts and leukoencephalopathy. Stroke 2005; 36: 2384–8.

Joutel A, Corpechot C, Ducros A, Vahedi K, Chabriat H, Mouton P, et al. Notch3 mutations in CADASIL, a hereditary adult-onset condition causing stroke and dementia. Nature 1996; 383: 707–10.

Jouvent E, Mangin JF, Porcher R, Viswanathan A, O'Sullivan M, Guichard JP, et al. Cortical changes in cerebral small vessel diseases: a 3D MRI study of cortical morphology in CADASIL. Brain 2008; 131 (Pt 8): 2201–8.

Kim JS, Yoon Y. Single subcortical infarction associated with parental arterial disease: important yet neglected sub-type of atherothrombotic stroke. Int J Stroke 2013; 8: 197–203.

Lammie GA, Wardlaw JM. Small centrum ovale infarcts–a pathological study. Cerebrovasc Dis 1999; 9: 82–90.

Lewis EB, Fox NC. Correction of differential intensity inhomogeneity in longitudinal MR images. Neuroimage 2004; 23: 75–83.

Maillard P, Fletcher E, Harvey D, Carmichael O, Reed B, Mungas D, et al. White matter hyperintensity penumbra. Stroke 2011; 42: 1917–22.

Maillard P, Carmichael O, Fletcher E, Reed B, Mungas D, DeCarli C. Coevolution of white matter hyperintensities and cognition in the elderly. Neurology 2012; 79: 442–8.

Mattes D, Haynor DR, Vesselle H, Lewellyn TK, Eubank W. Nonrigid multimodality image registration. In: Proceedings of SPIE. San Diego, CA, 2001.

O'brien JT, Erkinjuntti T, Reisberg B, Roman G, Sawada T, Pantoni L, et al. Vascular cognitive impairment. Lancet Neurol 2003; 2: 89–98.

O'sullivan M, Lythgoe DJ, Pereira AC, Summers PE, Jarosz JM, Williams SC, et al. Patterns of cerebral blood flow reduction in patients with ischemic leukoaraiosis. Neurology 2002; 59: 321–6.

Pantoni L, Garcia JH. Pathogenesis of leukoaraiosis: a review. Stroke 1997; 28: 652–9.

Pantoni L. Cerebral small vessel disease: from pathogenesis and clinical characteristics to therapeutic challenges. Lancet Neurol 2010; 9: 689–701.

Peters N, Opherk C, Bergmann T, Castro M, Herzog J, Dichgans M. Spectrum of mutations in biopsy-proven CADASIL: implications for diagnostic strategies. Arch Neurol 2005; 62: 1091–4.

Potter GM, Doubal FN, Jackson CA, Chappell FM, Sudlow CL, Dennis MS, et al. Counting cavitating lacunes underestimates the burden of lacunar infarction. Stroke 2010; 41: 267–72.

R Core Team. A language and environment for statistical computing. Vienna, Austria: R Foundation for Statistical Computing; 2012.

Salamon G, Corbaz JM. Atlas de la vascularisation artérielle du cerveau chez l'homme. Paris: Sandoz; 1971.

Schmidt R, Fazekas F, Kapeller P, Schmidt H, Hartung HP. MRI white matter hyperintensities: three-year follow-up of the Austrian Stroke Prevention Study. Neurology 1999; 53: 132–9.

Schmidt R, Enzinger C, Ropele S, Schmidt H, Fazekas F; Austrian Stroke Prevention Study. Progression of cerebral white matter lesions: 6-year results of the Austrian Stroke Prevention Study. Lancet 2003; 361: 2046–8.

Schmidt R, Ropele S, Enzinger C, Petrovic K, Smith S, Schmidt H, et al. White matter lesion progression, brain atrophy, and cognitive decline: the Austrian stroke prevention study. Ann Neurol 2005; 58: 610–6.

Schmidt R, Petrovic K, Ropele S, Enzinger C, Fazekas F. Progression of leukoaraiosis and cognition. Stroke 2007; 38: 2619–25.

Shih AY, Blinder P, Tsai PS, Friedman B, Stanley G, Lyden PD, et al. The smallest stroke: occlusion of one penetrating vessel leads to infarction and a cognitive deficit. Nat Neurosci 2013; 16: 55–63.

Smith SM, Jenkinson M, Woolrich MW, Beckmann CF, Behrens TE, Johansen-Berg H, et al. Advances in functional and structural MR image analysis and implementation as FSL. Neuroimage 2004; 23 (Suppl 1): S208–19.

Vemuri BC, Ye J, Chen Y, Leonard CM. Image registration via level-set motion: applications to atlas-based segmentation. Med Image Anal 2003; 7: 1–20.

Vermeer SE, Prins ND, Den Heijer T, Hofman A, Koudstaal PJ, Breteler MM. Silent brain infarcts and the risk of dementia and cognitive decline. N Engl J Med 2003; 348: 1215–22.

Viswanathan A, Guichard JP, Gschwendtner A, Buffon F, Cumurcuic R, Boutron C, et al. Blood pressure and haemoglobin A1c are associated with microhaemorrhage in CADASIL: a two-centre cohort study. Brain 2006; 129 (Pt 9): 2375–83.

Viswanathan A, Godin O, Jouvent E, O'Sullivan M, Gschwendtner A, Peters N, et al. Impact of MRI markers in subcortical vascular dementia: a multi-modal analysis in CADASIL. Neurobiol Aging 2010; 31: 1629–36.

Wardlaw JM, Sandercock PA, Dennis MS, Starr J. Is breakdown of the blood-brain barrier responsible for lacunar stroke, leukoaraiosis, and dementia? Stroke 2003; 34: 806–12.

Wardlaw JM. What is a lacune? Stroke 2008; 39: 2921–2.

Wardlaw JM, Smith C, Dichgans M. Mechanisms underlying cerebral small vessel disease: insights from neuroimaging. Lancet Neurol 2013; 12: 483–97.

Woolrich MW, Jbabdi S, Patenaude B, Chappell M, Makni S, Behrens T, et al. Bayesian analysis of neuroimaging data in FSL. Neuroimage 2009; 45 (Suppl 1): S173–86.

Zhu YC, Dufouil C, Mazoyer B, Soumaré A, Ricolfi F, Tzourio C, et al. Frequency and location of dilated Virchow-Robin spaces in elderly people: a population-based 3D MR imaging study. AJNR Am J Neuroradiol 2011; 32: 709–13.

Zieren N, Duering M, Peters N, Reyes S, Jouvent E, Hervé D, et al. Education modifies the relation of vascular pathology to cognitive function: cognitive reserve in cerebral autosomal dominant arteriopathy with subcortical infarcts and leukoencephalopathy. Neurobiol Aging 2013; 34: 400–7.